

## Research Article

# An Experimental Study on Settlement due to the Mutual Embedding of Miscellaneous Fill and Soft Soil

Fuhai Zhang <sup>1,2</sup>, Lei Zhang <sup>3</sup>, Tianbao Zhou,<sup>1,2</sup> Lijun Duan,<sup>1,2</sup> and Chong Shi<sup>1,2</sup>

<sup>1</sup>Key Laboratory of Ministry of Education for Geomechanics and Embankment Engineering, Hohai University, Nanjing 210098, China

<sup>2</sup>Research Institute of Geotechnical Engineering, Hohai University, Nanjing 210098, China

<sup>3</sup>School of Civil and Construction Engineering, Oregon State University, Corvallis, OR 97330, USA

Correspondence should be addressed to Lei Zhang; [zhanglei@oregonstate.edu](mailto:zhanglei@oregonstate.edu)

Received 4 December 2019; Accepted 10 February 2020; Published 4 March 2020

Academic Editor: Flavio Stochino

Copyright © 2020 Fuhai Zhang et al. This is an open access article distributed under the Creative Commons Attribution License, which permits unrestricted use, distribution, and reproduction in any medium, provided the original work is properly cited.

Settlement deformation in the foundation with miscellaneous fill and soft soil was typically calculated by summing up the settlement in each individual layer. However, this calculation method did not involve settlement deformation by embedding miscellaneous fill particles into soft soils under external loads, thus inducing significant settlement prediction error. To solve this problem, a laboratory testing device was developed to study the mutual embedding for specimens with different miscellaneous fill particle sizes, external loads, and particle materials. Testing results indicate that a larger particle size and subsequently the smaller specific surface resulted in greater mutual embedding settlement due to the smaller resistance. In addition, higher external loads and smaller interface friction both induced larger settlement. Based on these results, a theoretical calculation equation of settlement due to the mutual embedding of miscellaneous fill and soft soil was proposed. The calculated settlements were found to be well matching with the experimental results.

## 1. Introduction

Fast urbanization produces large amount of construction wastes which were used as foundation materials to fill lakes and wetlands of urban areas, providing new lands for urbanization. In these types of foundations, the surface soil layers are typically composed of multiphase bad-graded soils with complicated structures, so these types of foundations are called miscellaneous fill foundations. It sometimes contains waste fibers, gravels, and construction wastes with unevenly distributed density and loose structures, e.g., [1, 2]. The original bottom layers often contain saturated soft soils which may be easily squeezed into the voids between miscellaneous fill particles subjecting to overlying loads, and subsequently causing settlements of foundation (Figure 1). Nevertheless, existing theories of oedometric compression [3], plane strain [4], and three-directional compression [5] cannot interpret mutual embedding because the traditional methods of calculating total settlements can only consider settlements of miscellaneous fill layer and soft soil layer separately, e.g., [6–8],

neglecting settlement induced by mutual embedment of miscellaneous fill and soft soil. Currently, the studies of deformations of multimedia materials mainly focus on interface frictions including pile-soil frictional behaviors, e.g., [9–13], geotextile-soil frictional behaviors, e.g., [14–17] and pushing muds away from the road subgrade by throwing stones, e.g., [18–20]. There was no discussion of the mechanism of large particles embedding into soft soils under external loads. To study the mutual embedding behaviors, a new testing device was developed to investigate effects of external loads and miscellaneous fill particle characteristics (e.g., particle size and particle surface roughness) on mutual embedment deformation. Based on experimental results, a theoretical method of predicting mutual embedment settlement was proposed.

## 2. Experiment Setups

*2.1. Testing Device.* A mutual embedding experimental apparatus was designed according to mutual embedding

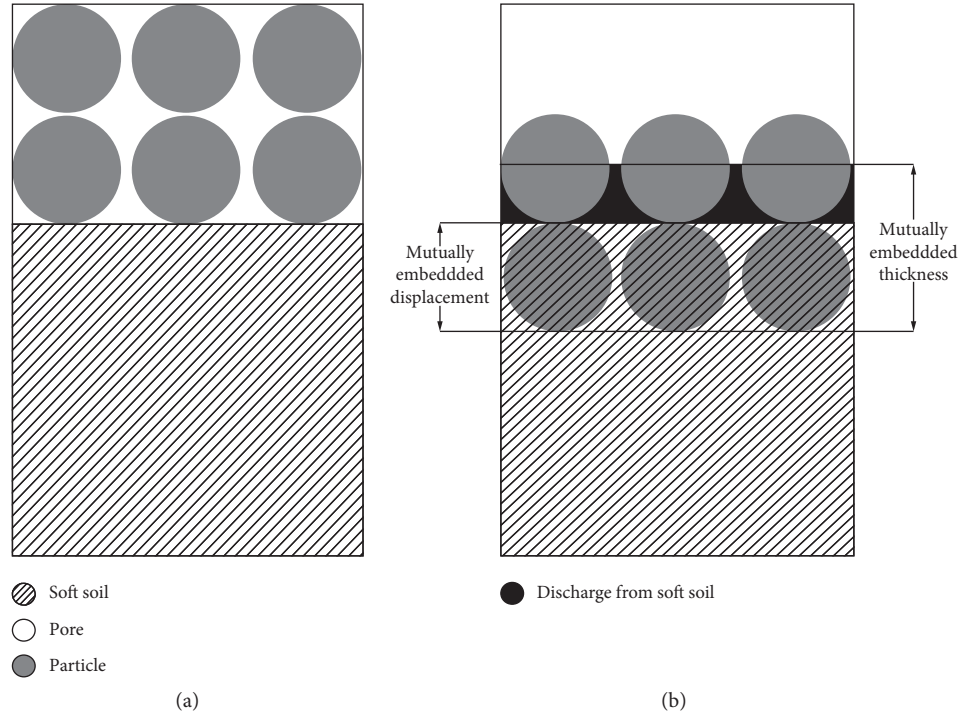


FIGURE 1: An example of mutual embedding of soft soil and miscellaneous fill particles: (a) before mutual embedding; (b) after mutual embedding.

deformation characteristics of miscellaneous fill and soft soil (Figure 2). This device was mainly composed of sample containers, a loading device, and a collector. The diameter of the containers was 30 cm, and the height of the containers was 40 cm. The device had upper and lower containers that were filled with miscellaneous fill and soft soil, respectively. The loading device provided a constant leverage loading. During the tests, the total volume of drainage water and total vertical displacement of the loading plate were recorded by a computer.

**2.2. Theory.** When the overlying pressure is smaller than or equal to 100 kPa, it can be assumed that 1. the container wall is stiff enough and there is only vertical deformation; 2. in the tests, miscellaneous fill particles are spherical and made of rigid materials in a very dense arrangement, so miscellaneous fill will not produce settlement deformation under low pressures which are lower than 100 kPa. Therefore, the total displacement ( $h$ ) only includes two components. One is the consolidation settlement ( $h_1$ ) of the soft soil layer, and the other is mutually embedding settlement ( $h_2$ ). According to the first assumption, the consolidation settlement of the soft soil layer can be calculated by measuring the drained water volume. Therefore,  $h_2$  can be calculated as

$$h_2 = h - h_1. \quad (1)$$

Then, the consolidation settlement can be calculated as

$$h_1 = \frac{V}{S}, \quad (2)$$

where  $V$  is the drained water volume and  $S$  is the sectional area of the sample container.

**2.3. Materials.** Soft soil was collected from the bed of Qinhuai River in Nanjing City with the particle size distribution, shown in Figure 3. Soil properties are listed in Table 1.

Miscellaneous fills with unique particle sizes were chosen as test samples. Effects of particle size and particle surface roughness on mutually embedding deformation were investigated. Five test groups were selected, including four groups of spherical cement particles with the diameters of 15 mm, 25 mm, 35 mm, and 45 mm (Figure 4). The last group of particles had spherical glass particles with the diameter of 25 mm. 25 kPa, 50 kPa, and 100 kPa of vertical loadings were applied to all the groups.

#### 2.4. Testing Procedures

**2.4.1. Test Preparation.** Spherical cement particles were cured for over 7 days, and filter papers and geotechnical cloth were stored in a box with the humidity of 100% for at least 48 h.

**2.4.2. Sample Installation.** First, a layer of geotechnical cloth was put on the bottom of the lower container, and a layer of filter papers was stuck onto the wall of the lower container (Figure 5(a)). Then, proper amount of water was added into the measuring burette with air discharged, and then the drainage valve was closed. Soft soil samples with a total

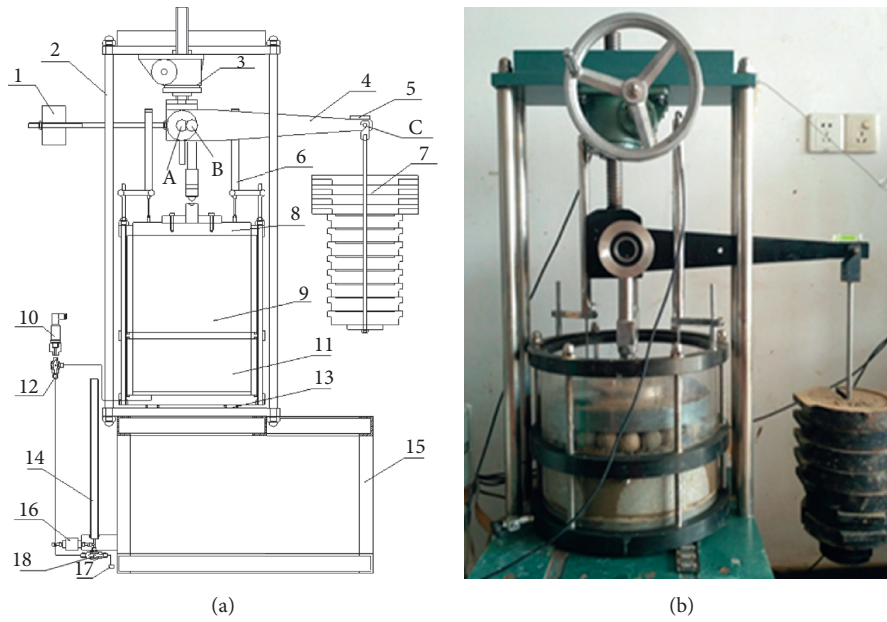


FIGURE 2: Mutual embedding testing apparatus: (a) design sketch; (b) photo picture. Note: different parts in (a) are numbered as follows: 1-counterforce weight; 2-counterforce framework; 3-leverage leveling structure; 4-leverage; 5-balancing bubble; 6-displacement sensor; 7-weights; 8-displacement plate; 9-upper contain; 10-pore pressure sensor; 11-lower container; 12-the first three-way valve; 13-ball row; 14-burette; 15-table support; 16-differential pressure sensor; 17-water vent; 18-the second three-way valve; A-pivot; B-force-bearing point; C-loading point.

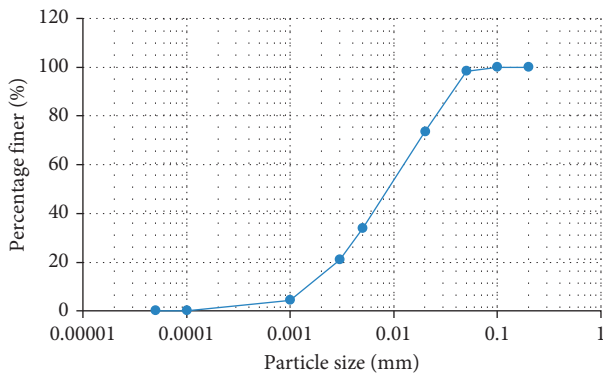


FIGURE 3: Particle size distribution of the soft soil.

height of 8 cm were filled into the container layer by layer with the height of about 2 cm in each layer. Four layers of soft soil were filled until the targeted height was reached (Figure 5(b)). In order to avoid air bubbles, soft soil was filled carefully in each layer, and after filling each layer, the sample was shaken by gently hitting the wall of the container with a hammer. Before filling the upper container, a thin layer of vaseline was coated onto the wall of the upper container. Particles were also filled in layer by layer from the broader to the center. The particle filling method is shown in Figure 5(c). After finishing the sample installation, the pressure plate was placed onto the sample top, and a bubble leveler was used to make sure the plate was leveled.

**2.4.3. Self-Weight Balance.** The self-weights of the pressure plate and particles may cause consolidation drainage of the

soft soil layer and mutual embedding. To avoid test error, self-weight balance must be performed. After the sample installation, the drainage valve on the lower container was opened for 12 hrs.

**2.4.4. Loading.** After the self-weight balance, the test program was started with the first step of resetting the displacement and differential pressure sensors. In the tests, loadings of 25 kPa, 50 kPa, and 100 kPa were applied with one loading in each test.

### 3. Analysis of Test Results

**3.1. Initial Test Data.** With equation (1), the mutual embedding settlement for specimens with different particle sizes of miscellaneous fill and different external loadings were calculated, shown in Figure 6. The mutual embedding settlement had three stages which were instantaneous deformation stage, continuous growth stage, and stable stage. The findings by comparing the results for specimens with different particle sizes, different external loadings, and different particle surface friction are discussed in the following sections.

**3.2. Effects of Miscellaneous Fill Diameter on Mutual Embedding Settlement.** From testing results in Figures 6 and 7, it can be seen that the mutual embedding settlement increases with increased spherical miscellaneous fill diameter regardless of the external loadings.

Different miscellaneous fill diameters will lead to different specific surface areas. Porosity values in the upper

TABLE 1: Physical and mechanical properties of test samples.

Natural moisture content	Void ratio	Plastic limit	Liquid limit	Specific gravity	Clay content	Organic content
40.2%	1.07	24.4%	41.9%	2.67	33.72%	3.08%

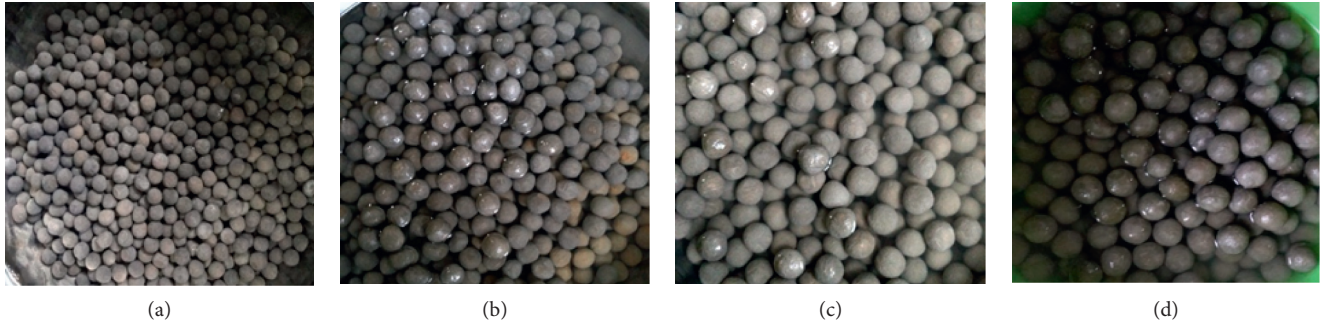


FIGURE 4: Miscellaneous fill materials with different particle sizes (spherical cement particles). (a) 15 mm. (b) 25 mm. (c) 35 mm. (d) 45 mm.

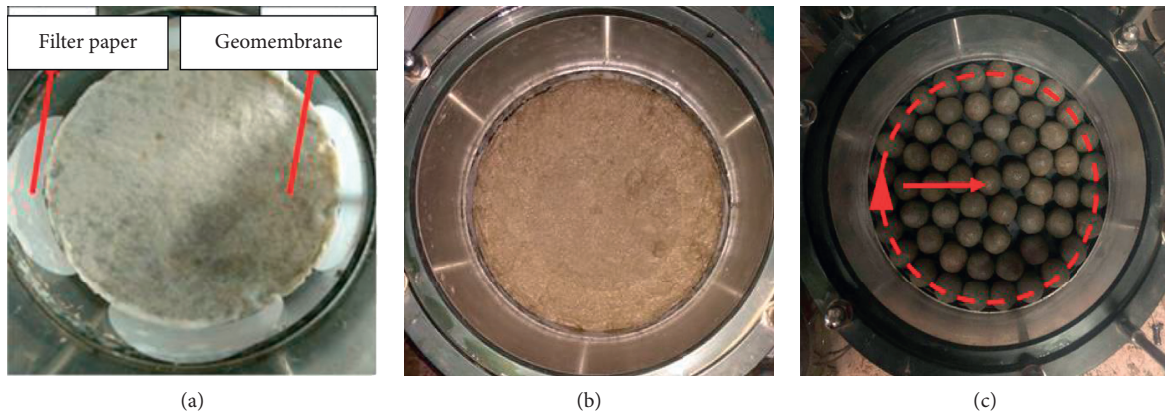


FIGURE 5: Sample installation processes: (a) installation of filter papers and the geomembrane; (b) clay layer; (c) cement particle filling process.

container filled with different diameters of miscellaneous fill particles were tested with the water-filling method, shown in Figure 8(a). Although porosities were increased with the increase of miscellaneous fill diameter, they were very close, ranging 0.43~0.45 which was very close to the maximum porosity of 0.4764 for simple cubic packing in three dimensions. However, different miscellaneous fill diameters can significantly change the specific surface area which is the total surface area of particles per unit volume (note: the specific surface area of spheres is  $6/d_i$ , where  $d_i$  is the diameter of spheres). Squeezing miscellaneous fill particles into soft soil was a process of shear deformation between miscellaneous fill particles and soft soil. With the increase of mutual embedding settlement, the total interface area between soft soil and miscellaneous fill particles was increased, and the constraint of soft soil over miscellaneous fill particles was also increased. The relationships between mutual embedding settlement and specific surface area of miscellaneous fill particles are plotted in Figure 8(b), showing that, with the increase of specific surface area, the mutual embedding settlement was decreased.

*3.3. Effects of External Loadings on Mutual Embedding Settlement.* The relationships between mutual embedding settlement and external loadings are plotted in Figure 9 for specimens with different miscellaneous fill particle sizes. It shows that the mutual embedding settlement increased with the increase of external loadings regardless of particle size. As mentioned above, the embedding process of miscellaneous fill particles into soft soil is a process of shear deformation between particles and soft soil, producing an upward frictional resistance. Mutual embedding settlement was stopped when the frictional resisting forces were able to balance the external loadings. Therefore, the shear deformation between particles and soft soil increased with external loadings, finally causing larger amount of mutual embedding settlement. In addition, the effect of increasing the external loadings on the mutual embedding settlement was more significant for samples with larger miscellaneous fill particles. This could be interpreted as that when the particle size was increased, the porosity shown in Figure 8(a) was increased, inducing smaller embedding resistance.

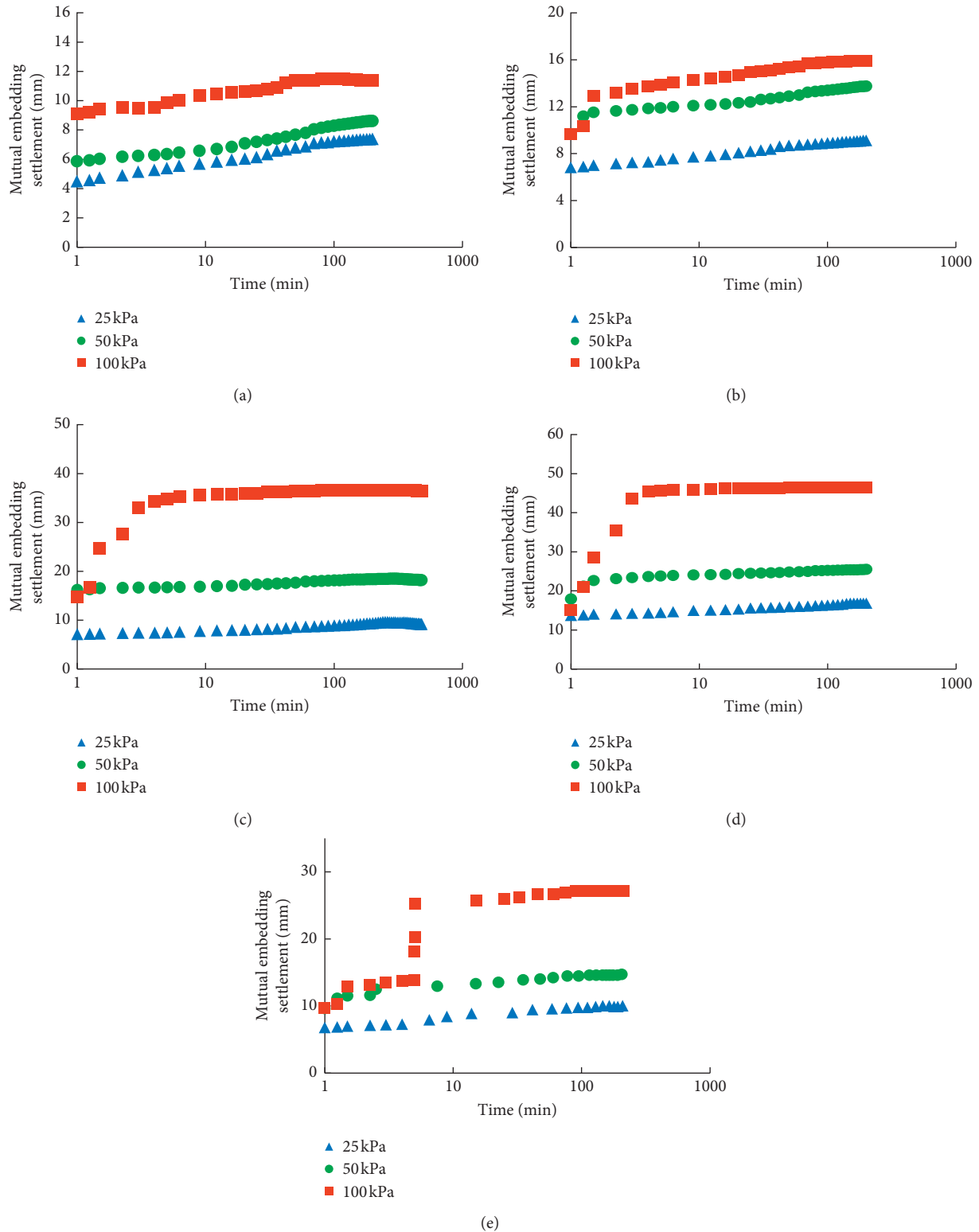


FIGURE 6: Mutual embedding settlement: (a) 15 mm cement balls; (b) 25 mm cement balls; (c) 35 mm cement balls; (d) 45 mm cement balls; (e) 25 mm glass beads.

3.4. *Effects of Particle Material on Mutual Embedding Settlement.* The shearing resistance on the interface between particles and soft soil supports the external loadings, so the interface friction can directly affect mutual embedding

settlement. Glass beads have smaller surface friction than that of the cement balls. The mutual embedding settlement for samples with these two types of balls is plotted in Figure 10. It can be seen that the samples with cement balls

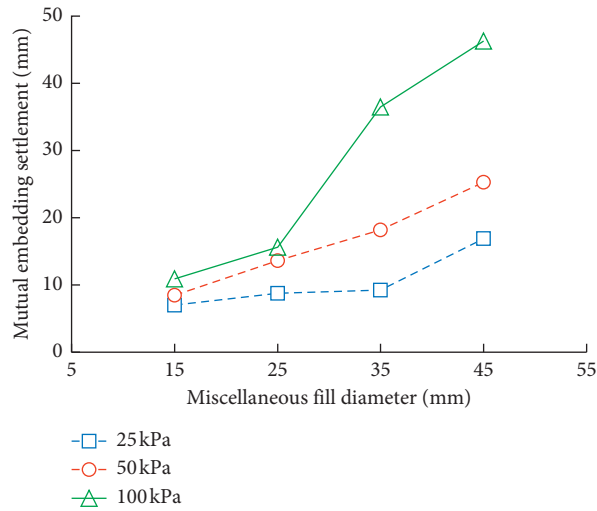


FIGURE 7: Relationship between the mutual embedding settlement and miscellaneous fill diameter.

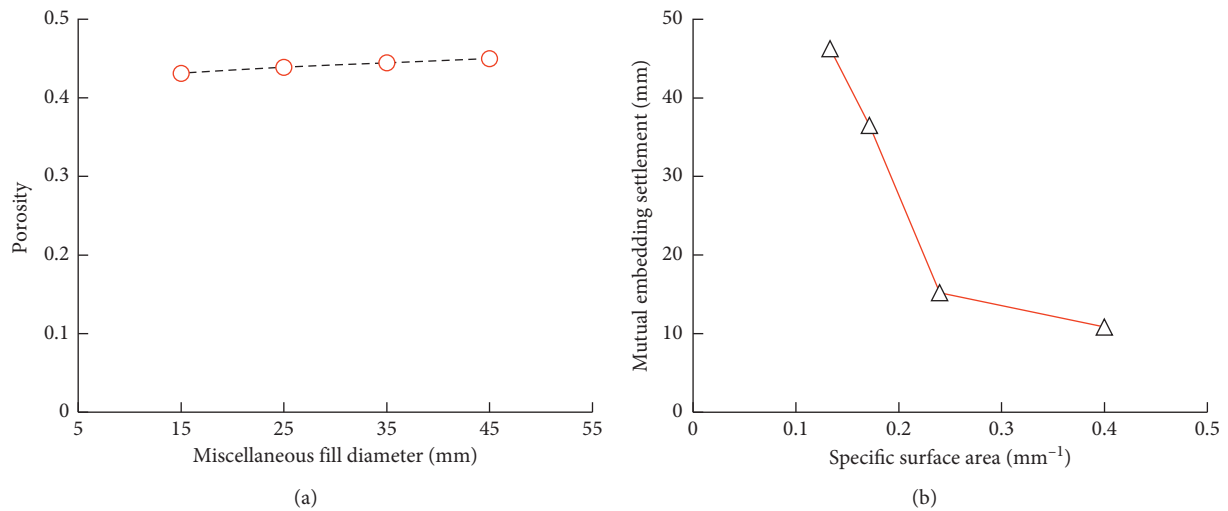


FIGURE 8: Effects of miscellaneous fill diameter on structural characteristics of miscellaneous fill: (a) relationship between porosity and miscellaneous fill diameter; (b) relationship between mutual embedding settlement and specific surface area of particles.

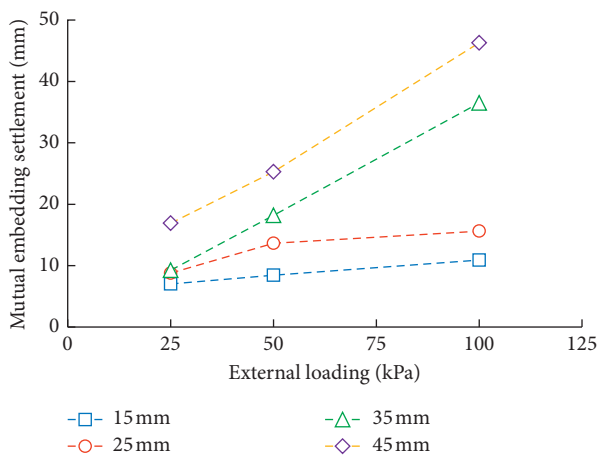


FIGURE 9: Effects of external loadings on mutual embedding settlement.

had higher interface friction which induced larger constraint over the interface and subsequently smaller mutual embedding settlement.

#### 4. Calculation of Mutual Embedding Settlement

4.1. Determine Interface Friction. With the application of external loadings, miscellaneous fill particles will be embedded into the soft soil, and shear deformation occurs on the interface, producing a resisting force. When the deformation is increasing, the resisting force is increasing by adding larger areas of interface between particles and soft soil. At the moment of the total shear force which equals to the external force, settlement will stop. Therefore, the relationship between the external loading and the shear strength will be as follows:

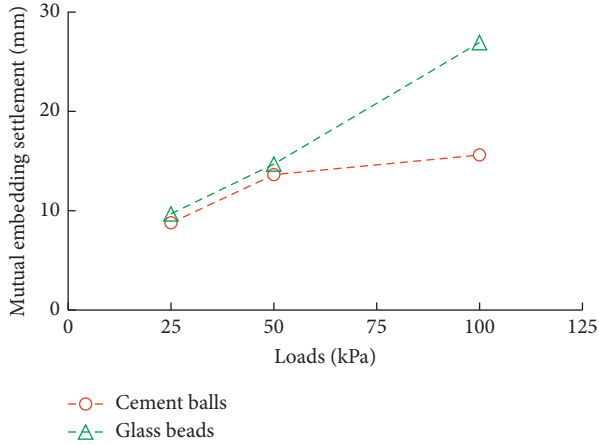


FIGURE 10: Effects of miscellaneous fill particle material on mutual embedding settlement.

$$P = \frac{\tau_f}{A_1}, \quad (3)$$

where  $P$  is the external loading (kN);  $\tau_f$  is the shearing resistance on the particle-soft soil interface, and  $A_1$  is the interface surface area. To calculate shearing resistance, the interface area ( $A_1$ ) in Figure 1 must be calculated, and it can be calculated with the mutual embedding settlement ( $h_2$ ). The calculation steps are as follows:

- (1) First, the volume and thickness of the mutual embedding layer ( $V_m$  and  $h_3$ ) shall be calculated. When the mutual embedding settlement is  $h_2$ , soft soil with a volume of  $V_1 = A \times h_2$  (where  $A$  is the sectional area of the container) is squeezed into miscellaneous fill voids. In other words, miscellaneous fill voids with a volume of  $V_v = V_1 = A \times h_2$  are filled up. Since the porosity of miscellaneous fill is  $n$ , the volume of the corresponding mutual embedding layer is  $V_m = (V_v/n) = (A \times h_2/n) = A \times h_3$ , where  $h_3$  is the thickness of the mutual embedding layer, and it values  $h_3 = h_2/n$  when there is no lateral deformation.
- (2) Second, the particle surface area ( $\bar{S}$ ) in a unit volume of miscellaneous fill should be calculated. For spherical miscellaneous fill particles with a diameter of  $d_i$ , the volume is  $V_i = \pi d_i^3/6$ , and the surface area is  $A_i = \pi d_i^2$ . Given the porosity of miscellaneous fill ( $n$ ), soil particle volume in a unit volume of miscellaneous fill is  $V_s = 1 - n$ , and the number of particles in a unit volume of miscellaneous fill is  $x = V_s/V_i$ . Therefore, the particle surface area in a unit volume of miscellaneous fill is  $\bar{S} = x \times A_i = (V_s/V_i) \times A_i$ .
- (3) The interface area ( $A_1$ ) in the mutual embedding layer is

$$A_1 = \bar{S} \times V_m = \frac{V_s}{V_i} \times A_i \times A \times \frac{h_2}{n} = \frac{(1-n)}{V_i} \times A_i \times A \times \frac{h_2}{n}. \quad (4)$$

Then, the external loading is

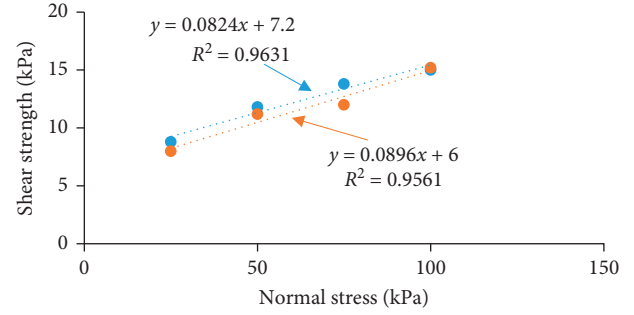


FIGURE 11: Shear strength versus normal stress in interface frictional behavior tests.

$$P = \tau_f \times A_1 = \tau_f \times \frac{(1-n)}{V_i} \times A_i \times A \times \frac{h_2}{n}. \quad (5)$$

**4.2. Particle-Soft Soil Interface Frictional Behavior Test.** A direct shear apparatus was used in this test. A piece of 10 mm thick cement plate or glass plate was placed into the lower shearing box. Soil samples were filled into the upper direct shear box to make the interface between upper and lower shearing boxes overlapping with the particle-soft soil interface. The overlying pressure was set to 25 kPa, 50 kPa, 75 kPa, and 100 kPa. Direct shear tests were under drained condition. During these tests, if the shear stress increased until a peak value followed with a decrease, the peak value was considered as the shear strength. If there was no decrease of shear stress, the value of shear stress when the shear displacement was at 4 mm was selected as the shear strength, and the shearing was stopped when the shear displacement reached 6 mm. Shear strengths are plotted in Figure 11. Shear strength parameters are listed in Table 2.

**4.3. Calculation of Mutual Embedding Settlement.** Given the external loading force,  $P$ ,  $P = p \times A$ , where  $p$  is the loading pressure (25 kPa, 50 kPa, and 100 kPa). According to equation (5), the mutual embedding settlement ( $h_2$ ) can be calculated as

$$h_2 = \frac{p \times A \times V_i \times n}{(\tau_f \times (1-n) \times A_i \times A)}. \quad (6)$$

Calculated results and test results are compared in Figure 12. It can be seen that the calculated mutual embedding settlements are able to well predict the test data for cement particle samples with different external loadings and for the glass bead sample.

## 5. Discussion

Miscellaneous fill medium has complicated composition, and the settlement of miscellaneous fill foundation is very special. Therefore, settlement of miscellaneous fill foundation caused by mutual embedding between sludge and miscellaneous fill under overlying loadings must be considered in the analysis of the settlement of miscellaneous fill

TABLE 2: Shear strength parameters of particle-soft soil interface frictional intensity.

Type of interface	Interface cohesion, $C_Q$ (kPa)	Interface friction angle, $\varphi_Q$ ( $^\circ$ )
Cement-soft soil interface	7.2	4.7
Glass-soft soil interface	6.0	5.1

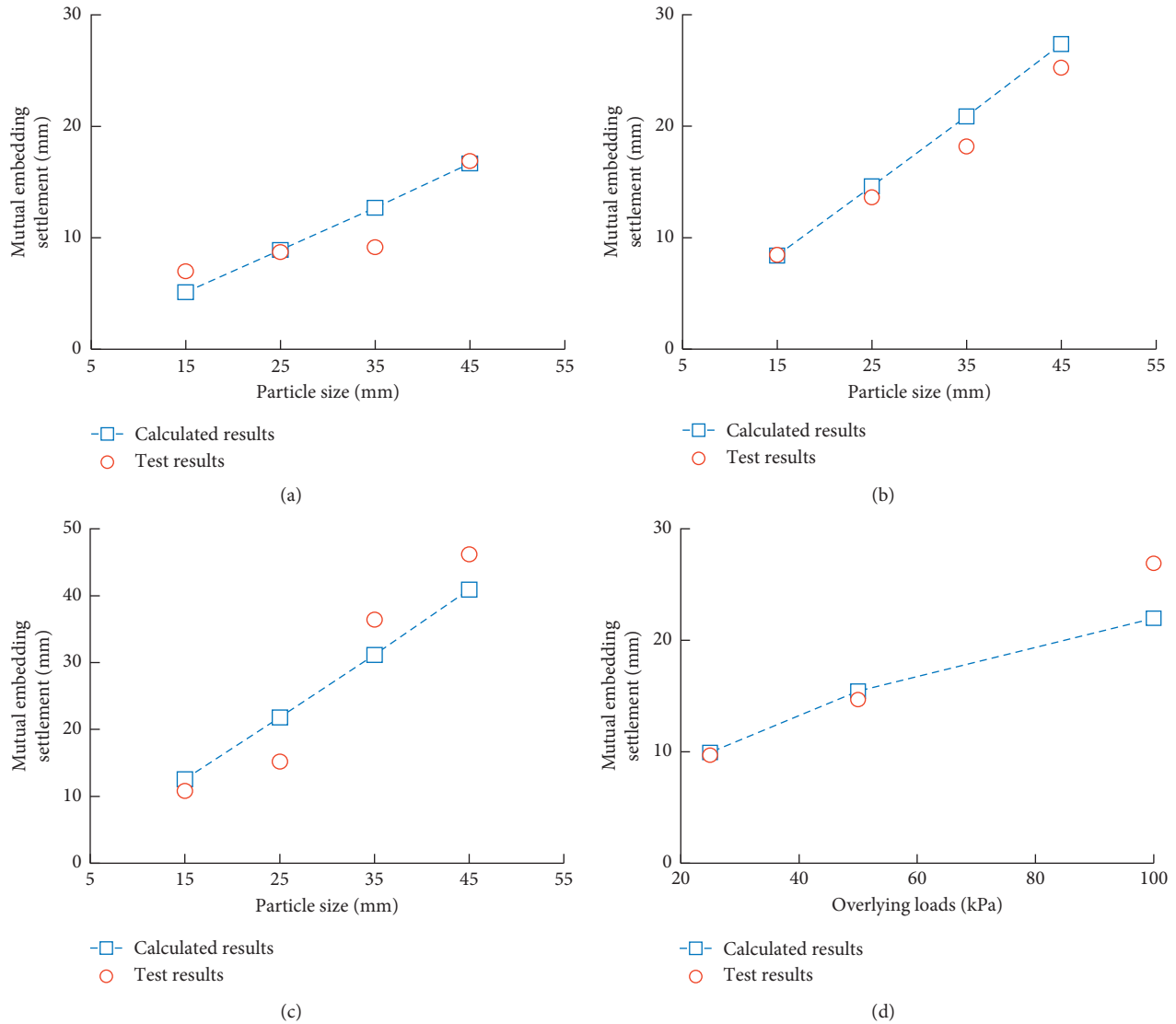


FIGURE 12: Comparison of calculated values with test results of mutual embedding settlement: (a) with 25 kPa external loading; (b) with 50 kPa external loading; (c) with 100 kPa external loading; (d) the sample with 25 mm glass beads.

foundation. Particle size, particle size distribution, material type, overlying loadings of miscellaneous fill, etc., can significantly affect mutual embedding settlement. There are few research studies on the mechanism of mutual embedding settlement between miscellaneous fill and soft soil. In this study, mutual embedding settlement was investigated through a self-made mutual embedding instrument. A theoretical equation of calculating the mutual embedding settlement between miscellaneous fill and soft soil was proposed based on experimental results and theoretical analysis results of frictional behaviors on the interface. This equation is applicable to calculate mutually embedded

settlement between the same size of miscellaneous fill and soft soil. However, further verifications are needed whether this equation is applicable to calculate mutual embedding settlement of miscellaneous fill foundation with complicated compositions and wide particle size distribution.

The self-made mutual embedding instrument has advantages of clear theory, easy operation, and reasonable testing data. Mutual embedding settlement is not directly measured, but it is calculated by equation (6). It is possible that assumption ② may cause testing error. The determination of 100 kPa in this assumption is based on that the depth of water like lakes in cities in the plain area in eastern

China is generally small (e.g., the average depth of Xuanwu Lake and Taihu Lake in Jiangsu Province in China is lower than 2 m), and the sum of overlying loadings including the filled soil weight and the traffic loadings is generally not higher than 100 kPa. According to miscellaneous fill compressive test results before mutual embedding process, when the external loading is smaller than 100 kPa, the settlement is negligible if the particles are arranged in a very dense manner. However, when the miscellaneous fill is loose, it is difficult to directly measure the settlement caused by the miscellaneous fill densification. Then, it is necessary to measure the miscellaneous fill settlement ( $h_4$ ) under the same loads as that in mutual embedding tests. Therefore, the mutual embedding settlement can be calculated as  $h_2 = h - h_1 - h_4$ . When the miscellaneous fill is loose or the external loading is large and settlement of miscellaneous fill cannot be overlooked, there might be testing error in the mutual embedding tests.

## 6. Conclusions

To investigate mutual embedding settlement between miscellaneous fill and soft soil under external loads, effects of particle size of miscellaneous fill, external loadings, and particle material on mutual embedding settlement are studied with a self-made mutual embedding device. A method of calculating the mutual embedding settlement was also proposed. Some major conclusions are as follows:

- (1) According to mutual embedding settlement tests with different particle sizes and materials, all curves of mutual embedding settlement versus time can be divided into three stages which are the instantaneous deformation stage, continuous growth stage, and stable stage.
- (2) Larger particle size leads to smaller specific surface area, inducing larger mutual embedding settlement. Larger external loadings induce larger shear deformation at the interface between miscellaneous particles and soft soil, and subsequently, larger mutual embedding settlement. Higher interface friction causes larger constraint on the interface, and the mutual embedding settlement is smaller.
- (3) Based on the theoretical analysis on mutual embedding settlement under interface friction, the theoretical calculation equation of mutual embedding settlement is proposed. The theoretical calculated results with this equation well match with the testing results. It achieves higher reasonability and reliability than the layered method does.

## Data Availability

The data used to support the findings of this study are included within the article.

## Conflicts of Interest

The authors declare that they have no conflicts of interest.

## Acknowledgments

This work was supported by the National Natural Science Foundation of China (NSFC no. 51778211) and the Natural Science Foundation of Jiangsu Province (Grant no: BK20171434).

## References

- [1] C. Shi, "Application of compound retaining system structured by anchor rod sheet piling and soil nailing retaining walls to deep pit of miscellaneous fill foundation," *Journal of Engineering Geology*, vol. 5, 2006.
- [2] J. P. Sun, G. B. Shao, and Z. B. Jiang, "Design and construction technology of displacement control in deep miscellaneous fill foundation pits," *Chinese Journal of Geotechnical Engineering*, vol. 34, no. S0, pp. 576–580, 2012.
- [3] M. Veiskarami, "Updated Lagrangian large deformation analysis of consolidation settlement with finite element method for a case study in Iran," *Scientia Iranica*, vol. 20, no. 4, pp. 1161–1174, 2013.
- [4] S. E. Aleksandrov and R. V. Goldstein, "Study of compression settlement of a three-layer rigid-plastic strip between parallel plates," *Mechanics of Solids*, vol. 49, no. 6, pp. 703–712, 2014.
- [5] B. Indraratna, A. S. Balasubramaniam, and N. Sivaneswaran, "Analysis of settlement and lateral deformation of soft clay foundation beneath two full-scale embankments," *International Journal for Numerical and Analytical Methods in Geomechanics*, vol. 21, no. 9, pp. 599–618, 1997.
- [6] W. S. Wang and J. Q. Yu, "Analysis on the Influence of the primary consolidation settlement of the  $e$ - $p$  curves and the soil bulk density of the soft soil foundation," *Advanced Materials Research*, vol. 919–921, pp. 645–648, 2014.
- [7] Z. Yu, C. Shanxiong, Y. U. Fei, X. Shudan, and D. Zhangjun, "Calculation method study of settlement process of high filling channels in south-to-north water diversion project," *Chinese Journal of Rock Mechanics and Engineering*, vol. 33, pp. 4367–4374, 2014.
- [8] F. Yu, Y. Zhang, S. Chen, and J. Yu, "Study on calculational methods for the settlement process of high filling canals," *Journal of Coastal Research*, vol. 73, pp. 108–115, 2015.
- [9] T. Nogami and M. Novak, "Soil-pile interaction in vertical vibration," *Earthquake Engineering & Structural Dynamics*, vol. 4, no. 3, pp. 277–293, 1976.
- [10] H.-b. Xiao, C.-s. Zhang, Y.-h. Wang, and Z.-h. Fan, "Pile-soil interaction in expansive soil foundation: analytical solution and numerical simulation," *International Journal of Geomechanics*, vol. 11, no. 3, pp. 159–166, 2011.
- [11] W. Cao, Y. Chen, and W. E. Wolfe, "New load transfer hyperbolic model for pile-soil interface and negative skin friction on single piles embedded in soft soils," *International Journal of Geomechanics*, vol. 14, no. 1, pp. 92–100, 2013.
- [12] M. Zhao and W. P. Cao, "An analysis of pile-soil interaction under embankment load," *Applied Mechanics and Materials*, vol. 488–489, pp. 458–461, 2014.
- [13] H. Zhou, G. Kong, and Z. Cao, "Theoretical analysis on pile-soil interaction of tapered pile under lateral load," *Journal of Central South University*, vol. 47, no. 3, pp. 897–904, 2016.
- [14] C. Chen, G. R. McDowell, and N. H. Thom, "Discrete element modelling of cyclic loads of geogrid-reinforced ballast under confined and unconfined conditions," *Geotextiles and Geomembranes*, vol. 35, pp. 76–86, 2012.
- [15] H.-l. Wang, W.-y. Xu, and F. Zhu, "The mechanical response of piles with consideration of pile-soil interactions under a

- periodic wave pressure,” *Journal of Hydrodynamics*, vol. 26, no. 6, pp. 921–929, 2014.
- [16] V. J. Vineetha and K. Ganesan, “Interface friction between glass fibre reinforced polymer and gravel soil,” *Advanced Materials Research*, vol. 984-985, pp. 707–710, 2014.
- [17] J. Q. Wang, Y. F. Zhou, Y. Xia, and S. B. Huang, “Development and application of new visual pullout test apparatus for geosynthetics,” *Chinese Journal of Geotechnical Engineering*, vol. 38, no. 4, pp. 718–725, 2016.
- [18] N. Karajan, O. Röhrle, W. Ehlers, and S. Schmitt, “Linking continuous and discrete intervertebral disc models through homogenisation,” *Biomechanics and Modeling in Mechanobiology*, vol. 12, no. 3, pp. 453–466, 2013.
- [19] J. T. Cai, “Pull-out test on interface behavior between expansive soils and geogrids,” *Rock & Soil Mechanics*, vol. 36, no. S1, pp. 204–208, 2015.
- [20] C. Shi and S.-l. Liu, “An underwater stress-testing technique for the heavy-hammer tamping of a rubble-mound foundation,” *Advances in Mechanical Engineering*, vol. 10, no. 1, Article ID 168781401875495, 2018.